DOI: 10.1002/chem.200903279

Colloidal Noble-Metal and Bimetallic Alloy Nanocrystals: A General Synthetic Method and Their Catalytic Hydrogenation Properties

Shuyan Song,[a] Ruixia Liu,[b] Yu Zhang,[a] Jing Feng,[a] Dapeng Liu,[a] Yan Xing,[a] Fengyu Zhao,[b] and Hongjie Zhang*[a]

Abstract: A general single-step strategy has been developed for the direct thermal decomposition of noble-metal salts in octadecylamine to synthesize octahedron- and rod-shaped noble-metal aggregates and monodisperse noble-metal or bimetallic alloy nanocrystals without introducing any additive into the system. It has presented a facile and economic way to fabricate these nanocrystals, especially alloy nanocrystals, which does not require a post-synthesis solid-state annealing process. The morphology of the nanocrystals can be easily controlled by tuning the synthetic temperature. Their ability to catalyze heterogeneous Suzuki coupling reactions has been investigated and showed satisfactory catalytic activity. The catalytic performance of the monometallic and bimetallic alloy nanocrystals were also evaluated in the selective hydrogenation of citral in a conventional organic solvent (toluene) and a green solvent (supercritical carbon dioxide, $scCO_2$). Interestingly, the catalysts performed differently to each other when they were in $scCO_2$ owing to the different morphology, which should be readily optimized for further use.

Keywords: alloys · catalysis · gold · nanocrystals · palladium · platinum

Introduction

The development of uniform colloidal metallic nanocrystals has been intensively explored because of their technological and fundamental scientific importance.[1–3] Among them, noble-metal nanocrystals often exhibit wide applications, especially catalytic properties, including heterogeneous transformations and homogeneous catalysis, which cannot be achieved by their bulk counterparts.[4–13] There have been numerous types of reactions that have been catalyzed by using colloidal noble-metal nanocrystals, particularly palladium and platinum, such as oxidations, cross-coupling reactions, electron-transfer reactions, hydrogenations, fuel-cell reactions, and many others.[14–20] Also, noble-metal alloy nanocrystals are of significant interest as electrocatalysts and selective oxidation and dehydrogenation catalysts.[21–24] On the other hand, noble-metal nanocrystals composed of multiple elements are of significant interest from both technological and scientific points of view for improving the activity and properties of catalysts.[25–28] However, the synthesis of homogeneous alloy samples still remains a challenge because they are, in principle, immiscible and hence phase segregation seems to be unavoidable. It is well known that the properties of noble-metal nanocrystals strongly depend on their surface properties.[29] The activity and selectivity of nanoparticles (NPs) can, therefore, be tuned by controlling the morphology because the exposed surfaces of the particles have distinct crystallographic planes depending on the shape.[30] Increasingly, the shape, size, composition, and architecture are being recognized as important control parameters in the tailoring of noble-metal nanostructure systems.

There have been extensive efforts focusing on the development of new synthetic methodologies for the synthesis of noble-metal nanocrystals such as seed-mediated growth, photochemical reduction, template-directed synthesis, and electrochemical deposition.[31–38] Among the various wet-chemical approaches that have been developed for the preparation of colloidal noble-metal nanocrystals, the reduction of metal salts is the most common because this method offers a variety of parameters that can influence the physical and chemical properties of the resulting materials, and reducing agents such as hydrogen, hydrazine, alcohols, carbon

[a] Dr. S. Song, Y. Zhang, J. Feng, D. Liu, Y. Xing, Prof. H. Zhang
State Key Laboratory of Rare Earth Resource Utilization
Changchun Institute of Applied Chemistry
Changchun 130022 (P.R. China)
Fax: (+86) 431-8569-8041
E-mail: hongjie@ciac.jl.cn

[b] Dr. R. Liu, Prof. F. Zhao
State Key Laboratory of Electroanalytical Chemistry
Changchun Institute of Applied Chemistry
Changchun 130022 (P.R. China)

monoxide, $LiAlH_4$, $NaBH_4$, or $R_4N^+(Et_3BH^-)$ have been used to prepare metal colloids in the nanometer size range.[39–46] For example, monodisperse gold nanoparticles were produced by the single-phase reduction of $AuPPh_3Cl$ with an amineborane complex in the presence of an alkyl thiol.[19] Teranishi and Miyake synthesized monodisperse Pd nanoparticles by heating H_2PdCl_4 at reflux in a mixture of water and various alcohols in the presence of polyvinylpyrrolidone (PVP).[47] Hyeon and co-workers synthesized monodisperse 3.5 nm sized Pd nanoparticles by thermal decomposition of a Pd–trioctylphosphine (TOP) complex in TOP.[34] However, the use of these additives may introduce heterogeneous impurities. Although additives can direct the growth of noble-metal nanocrystals with controlled morphologies and architectures, post-synthetic treatments are needed to remove any additives from the products, which might destroy the nanocrystals. Therefore, developing a facile, general, and inexpensive method to prepare noble-metal nanoparticles with controlled shape and size still remains a great challenge, which is of interest and importance for their further applications. Herein, we have developed a general single-step strategy for the direct thermal decomposition of noble-metal salts in octadecylamine (ODA) to synthesize octahedron- and rod-shaped noble-metal aggregates and noble-metal or bimetallic nanocrystals, which does not require any additive in the system. ODA molecules perform three roles in the reaction, namely, solvent, reductant, and capping agent. Their ability to catalyze heterogeneous Suzuki coupling reactions and the hydrogenation of unsaturated organics have also been investigated and show satisfactory performance.

Results and Discussion

The XRD patterns of the products are shown in Figure 1. The six samples (Au NPs, Pd NPs, Pt NPs, AuPd alloy NPs, AuPt alloy NPs, and Pt nanorod aggregates) present similar profiles and no impurities are discernible. Note that no phase segregation was detected in the alloy samples, but for the alloy sample (AuPd) synthesized at high temperature, obvious phase segregation was observed in the XRD pattern (Figure 2). It can be seen from Figure 1 that the 2θ values of

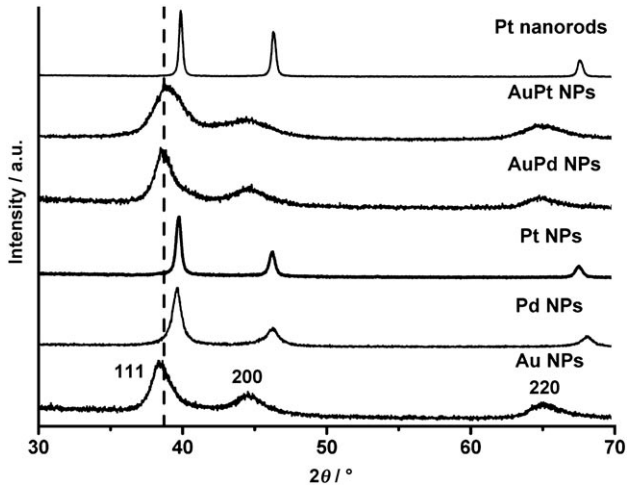

Figure 1. XRD patterns for noble-metal and alloy nanocrystals.

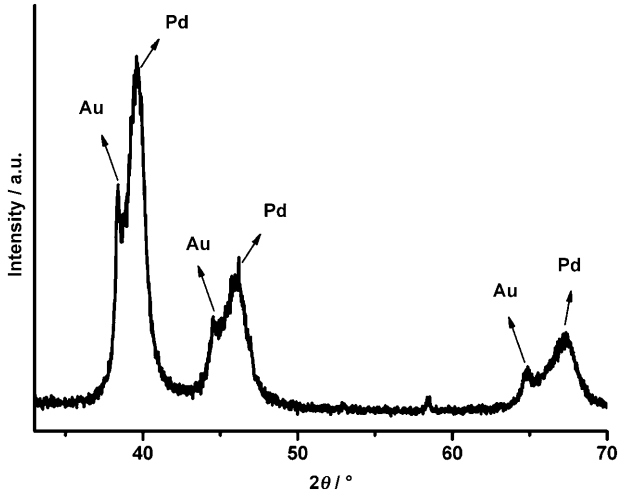

Figure 2. XRD pattern of the phase-segregated alloy sample (AuPd) synthesized at high temperature.

the XRD signals gradually shift towards higher angles with increasing the ratio of Au to Pt, which indicates that the lattice constants and cell volumes shrink. Transmission electron microscopy (TEM) and high-resolution TEM (HRTEM) were applied to study the morphology and size of the product obtained by the thermolytic process employed here. Figure 3 shows the TEM images of noble-metal and noble-metal alloy nanocrystals, from which we can see that Au, Pd, Pt, AuPd alloy and AuPt alloy are monodisperse NPs, with an average size of 7.0 nm. The high-temperature (330 °C) thermolytic products of $H_2PtCl_6{\cdot}6H_2O$ are monodisperse nanorod aggregates that are built up from uniform nanorods with diameters of 6.0 nm and lengths of 40 nm. A typical individual Pt nanorod aggregate with a diameter of 80 nm is shown in Figure 4 f, and is composed of several hundreds of nanorods. From their HRTEM images (Figure 4), it can be clearly seen that these nanoparticles are well crystallized and have a typically octahedral structure with the (111) planes exposed outside. The clear lattice fringes with an interplanar distance ranging from 2.3 to 2.2 Å is a characteristic fringe spacing of the cubic crystal phase in the (111) plane. The HRTEM image taken from a single rod (Figure 4 f, inset) shows that the nanorod is structurally uniform with a clearly resolved interplanar spacing of about 2.2 Å, which can be indexed to the (111) planes, and that the axis of the nanorod is along the [100] direction.

Based on the above experimental results, the growth mechanism and relationship between the reaction conditions and the morphology and size of final products can be con-

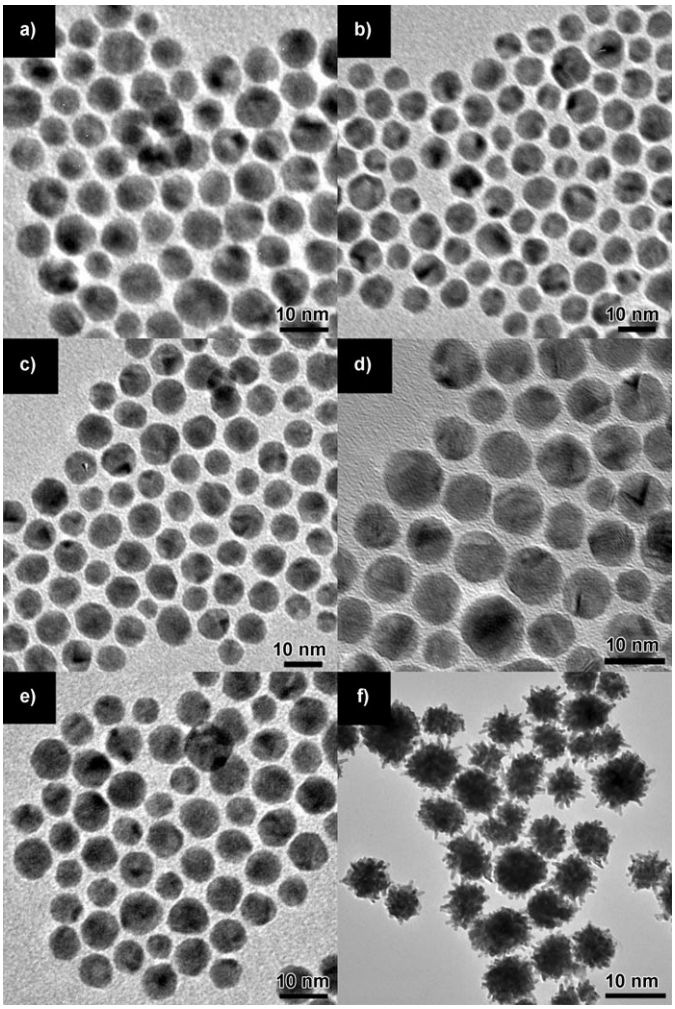

Figure 3. TEM images for noble-metal and alloy nanocrystals: a) Au NPs, b) Pd NPs, c) Pt NPs, d) AuPd alloy NPs, e) AuPt alloy NPs, and f) Pt nanorod aggregates.

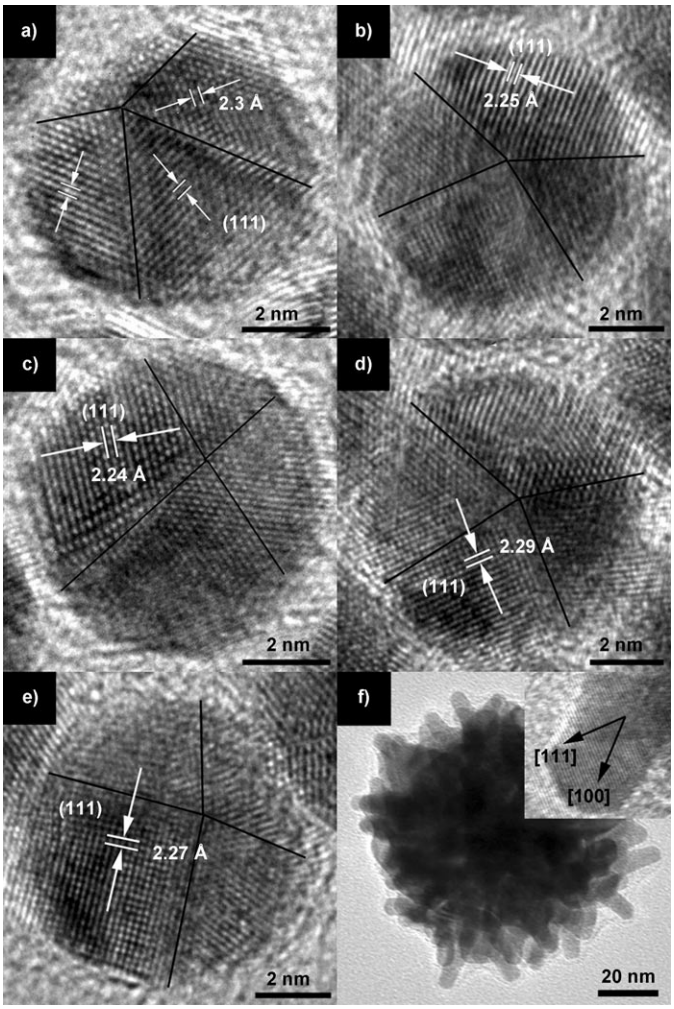

Figure 4. HRTEM images for noble-metal and alloy nanocrystals: a) Au NPs, b) Pd NPs, c) Pt NPs, d) AuPd alloy NPs, e) AuPt alloy NPs, and f) Pt nanorod aggregates.

cluded. It is reported that there are two critical factors responsible for the determination of the morphology of the nanocrystals, that is, the nucleation process and the subsequent growth stage. In the nucleation process, uniform noble-metal nuclei and their alloy nuclei form when the reactants are placed into hot octadecylamine and the crystalline phase of the seeds is very important for directing the intrinsic morphology of nanocrystals. In the growth stage, the delicate control of the growth conditions can govern the final architecture of the nanocrystals. Octahedron- and rod-shaped noble-metal aggregates and their alloy nanocrystals can be obtained through the change of the growth temperature. Surface-energy and kinetic considerations are taken into account to understand the formation mechanisms of the single-crystalline noble-metal and their alloy nanocrystals with varying shapes. The solvent molecules, ODA, are found to alter the surface energies of metal facets in the order $\{100\} > \{110\} > \{111\}$ under the growth conditions, whereas the growth kinetics leads to the formation of thermodynamically less favored shapes that are not bound by the most stable facets. This result is consistent with those of reports that adsorbates (including surfactants, polymers, small molecules, and atomic adsorbates) can selectively interact with different metal crystal facets and alter their surface energies in the order $\gamma\{111\} < \gamma\{100\} < \gamma\{110\}$ in a solution-phase synthesis. Therefore, octahedral nanocrystals are formed when the capping of ODA on {111} facets dominates. While at higher temperature, the system will have sufficient thermal energy. The solvent molecules move so fast that the interaction between ODA and the nuclei become weak, which leads to a high concentration of the free nuclei. According to the theory proposed by Peng et al., the high monomer concentration is beneficial for the formation of elongated nanocrystals.[48] As a result, the environment with a higher chemical potential accelerated the oriented growth, leading to the formation of 1D Pt nanorods. In addition, the as-synthesized Pt nanorods possessed high surface energy and were unstable in such high-temperature systems. Driven by minimization of the energy of the system, the nanorods came together to form nanorod aggregates.

In a further set of experiments, the Suzuki cross-coupling reaction of benzene halides and phenylboronic acid was selected as a test reaction by using Pd NPs as the catalyst (3 mol%) in ethanol under reflux conditions. As an example reaction, the addition of phenylboronic acid to a mixture of iodobenzene, potassium phosphate, and the Pd NPs in ethanol provided biphenyl products in an almost quantitative conversion after 5 h under reflux conditions. When phenylbromides were used as the reactant instead of iodobenzene, five times more Pd NP catalyst was required to achieve a similar yield. The reaction with chlorobenzene did not proceed, showing that the Pd NPs are not active enough to catalyze the reaction. The as-synthesized Pd NPs also show high catalytic activity in the reaction between benzene diiodide and thiophene diiodide with phenylboronic acid. Table 1 shows the conversion for the reaction of various benzene halides and phenylboronic acid when using the Pd NPs. The high catalytic activity may be attributed to the high surface area of the small-size nanocrystals and their good monodispersion.

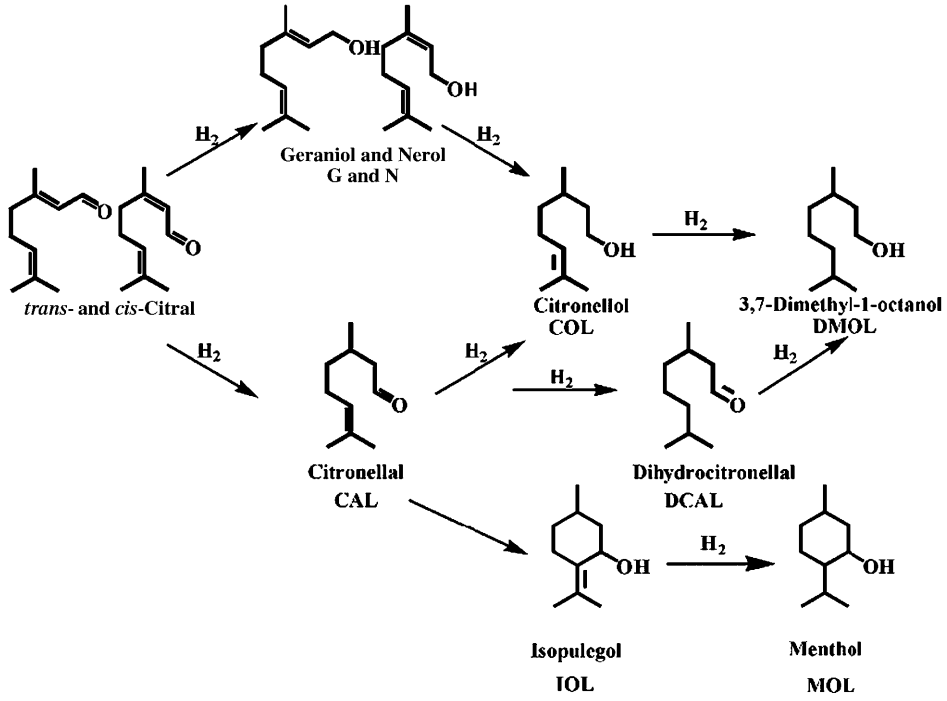

Scheme 1. The hydrogenation of citral.

The catalytic performances of the mono- and bimetallic alloy nanocrystals were also evaluated in the selective hydrogenation of citral in a conventional organic solvent (toluene) and in supercritical carbon dioxide ($scCO_2$). Selective hydrogenation of citral is an important reaction in the flavor, fragrance, and pharmaceutical industries.[49] The reaction pathways of the hydrogenation of citral are complicated, giving various products such as citronellal, citronellol, geraniol, nerol, menthol, and others through hydrogenation reactions of the C=C and C=O bonds involved (Scheme 1). It is, therefore, important to control the product selectivity as well as the overall conversion in the citral hydrogenation, and thus it was selected as a model reaction for testing the performance of catalysts.[50] The results of hydrogenation reactions are presented in Table 2.

When the reaction took place in the conventional solvent toluene, the conversion of citral over the Pt NPs was 44%, whereas it was two times that conversion over the Pt nanorod aggregates (89%). It indicated that the morphology of the catalysts have a great effect on the catalytic performance. Compared with the monometallic Pt NPs that have a similar size, the conversion was dramatically increased over the bimetallic AuPt alloy NPs, which maybe attributed to the electronic and geometric effect as reported in the literature.[51,52] The selectivity to unsaturated alcohols (G and N) was very low (4%) over the monometallic Pt (NPs and nanorod aggregates). However, it increased up to 35% over the bimetallic AuPt alloy, which is larger by a factor of eight relative to the monometallic Pt. The presence of Au facilitated the hydrogenation

Table 1. Results from the Suzuki cross-coupling reactions for various substrates.

Entry	Benzene halides	Time [h]	Product	Conversion [%]
1	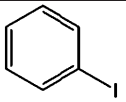	5	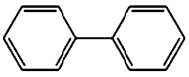	99
2	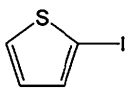	5	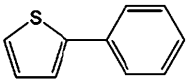	96
3	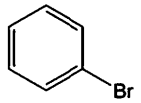	24	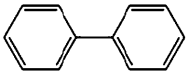	91
4		24	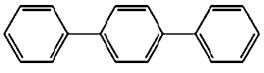	95

Table 2. Hydrogenation of citral over monometallic (Pt) and alloy (AuPt) nanocrystals.[a]

Entry	Catalysts	Conversion [%]	Selectivity [%]					
			DCAL	CAL	IOL	DCOL	COL	G and N
			Toluene[b]					
1	Pt NPs	44	7	43	18	4	24	4
2	Pt nanorods	89	16	26	14	16	23	4
3	AuPt NPs	55	3	29	7	3	23	35
			$scCO_2$[c]					
4	Pt NPs	82	13	39	10	8	28	4
5	Pt nanorods	79	12	28	12	11	31	7
6	AuPt NPs	46	2	18	3	12	0	59

[a] Reaction conditions: citral (2 mmol), H_2 (3 MPa), 80 °C, 4 h. The quantity of the catalysts in toluene was two times higher than in $scCO_2$. [b] Toluene (5 mL), catalyst (10 mg). [c] CO_2 (8 MPa), catalyst (5 mg).

of the C=O bond. It was reported that nanoparticulate Au was intrinsically selective to unsaturated alcohols when it was used to catalyze the hydrogenation of unsaturated aldehydes, for example, 95% of the selectivity to G and N was obtained over Au/Fe_2O_3 in ethanol for the hydrogenation of citral.[50]

Interestingly, it was found that different catalytic performance appeared in $scCO_2$ over the same catalysts. It can be seen that the conversions of citral over Pt NPs and Pt nanorod aggregate catalysts were similar, about 80% (Table 2, entries 4 and 5), and the conversion over the AuPt alloy NPs (46%) was much lower than that over the monometallic Pt NPs under the same condition used. The selectivity to unsaturated alcohols (G and N) was 4 and 7% for the monometallic Pt NPs and nanorod aggregates, respectively. It sharply increased up to 56% for the AuPt alloy NPs, which was much larger than in toluene. This indicates that compared with the conventional organic solvent toluene, the activity in the green solvent $scCO_2$ was much higher owing to the high mass-transfer rate and complete miscibility with the reactants (H_2 and citral),[53] because half the quantity of the catalyst was used in $scCO_2$. The interaction between molecular CO_2 with C=O in citral was responsible for the higher selectivity to G and N in $scCO_2$ as reported in our previous work.[54–57]

Conclusion

In summary, a general single-step strategy for the direct thermal decomposition of noble-metal salt in octadecylamine to synthesize various noble-metal or bimetallic alloy nanocrystals has been described. It presented a facile and economic way to fabricate such nanocrystals with different morphologies, which does not require a post-synthesis solid-state annealing process or the addition of any additive. Their ability to catalyze heterogeneous Suzuki coupling reactions and the hydrogenation of unsaturated organics has been investigated and showed satisfactory catalytic activity. Through morphology control and surface modification, the catalytic properties of these monodisperse nanocrystals should be readily optimized for further use.

Experimental Section

General methods and materials: $HAuCl_4{\cdot}4H_2O$, $PdCl_2$, and $H_2PtCl_6{\cdot}6H_2O$ were purchased from Sinopharm Chemical Reagents. ODA (>90%) was obtained from Aldrich. All other reagents were used without further purification.

X-ray powder diffraction patterns of the samples were collected on a Rigaku D_{max} 2000 X-ray diffractometer with $Cu_{K\alpha}$ radiation (λ = 0.154178 nm) with 2θ ranging from 30 to 70°. TEM images, HRTEM images and selected area electron diffraction (SAED) patterns were obtained on a JEOL JEM-2100 field-emission microscope with an accelerating voltage of 200 kV.

Synthesis: In a typical synthesis of monodisperse Au NPs (7.0 nm), $HAuCl_4{\cdot}4H_2O$ (1 mmol) was added to hot ODA (13.5 g, 10 mmol) at 180 °C in the three-necked flask. This temperature was maintained for 1 h under magnetic stirring for further growth and crystallization before being cooled to 50 °C. Excess ethanol was added to precipitate the Au NPs, which were washed with hexane and ethanol several times. The Au NPs could be redispersed in many organic solvents such as hexane, toluene, and chloroform.

When $PdCl_2$ or $H_2PtCl_6{\cdot}6H_2O$ (1 mmol) was introduced in the reaction instead of $HAuCl_4{\cdot}4H_2O$, Pd and Pt NPs were obtained. The synthetic procedure for the synthesis of AuPd and AuPt alloys was very similar to that of Au, Pd, and Pt NPs, but $HAuCl_4{\cdot}4H_2O$ (0.5 mmol), $PdCl_2$ (0.5 mmol), $HAuCl_4{\cdot}4H_2O$ (0.5 mmol), or $H_2PtCl_6{\cdot}6H_2O$ (0.5 mmol) were used. Pt nanorod aggregates were obtained when the reaction temperature was 330 °C.

Catalytic performance: The catalytic performance of the noble-metal nanocrystals and alloys were tested for the selective hydrogenation of citral. The reaction was carried out in a stainless-steel batch reactor (50 cm^3). The desired amounts of citral and the catalysts were added into the reactor, which was then sealed and flushed with N_2 more than three times. The reactor was heated to 80 °C and first H_2 (3 MPa) and then CO_2 (8MPa) were added with a high-pressure liquid pump. The reaction was started with continuous agitation. At the end of reaction, the reactor was cooled to room temperature and the gases (H_2 and/or CO_2) were vented. Finally, the reaction mixture was extracted with *n*-hexane. The resulting solutions were analyzed with gas chromatography (GC-Shimadza-14C, FID; capillary column Rtx-Wax 30 m × 0.53 mm × 0.25 mm) and gas GC–MS (Agilent 5890). For the reaction runs in toluene, the same procedure was used except for the introduction of CO_2.

Acknowledgements

The authors are grateful to the financial aid from the National Natural Science Foundation of China (Grant Nos. 20631040 and 20610102007) and the MOST of China (Grant Nos. 2006CB601103 and 2006DFA42610).

[1] L. Yu, I. A. Banerjee, M. Shima, K. Rajan, H. Matsui, *Adv. Mater.* **2004**, *16*, 709.
[2] R. Narayanan, M. A. El-Sayed, *J. Phys. Chem. B* **2005**, *109*, 12663.
[3] T. Hanrath, B. A. Korgel, *Adv. Mater.* **2003**, *15*, 437.
[4] S. A. Yeung, R. Hobson, S. Biggs, F. Grieser, *Chem. Commun.* **1973**, 378.
[5] J. Zheng, Y. Ding, B. Z. Tian, Z. L. Wang, X. W. Zhuang, *J. Am. Chem. Soc.* **2008**, *130*, 10472.

[6] J. Park, J. Joo, S. G. Kwon, Y. Jang, T. Hyeon, *Angew. Chem.* **2007**, *119*, 4714; *Angew. Chem. Int. Ed.* **2007**, *46*, 4630.
[7] Y. J. Xiong, Y. N. Xia, *Adv. Mater.* **2007**, *19*, 3385.
[8] C. Tsung, J. N. Kuhn, W. Huang, C. Aliage, G. A. Somorjai, P. D. Yang, *J. Am. Chem. Soc.* **2009**, *131*, 5816.
[9] Z. Huo, F. Tsung, W. Huang, X. Zhang, P. D. Yang, *Nano Lett.* **2008**, *8*, 2041.
[10] S. J. Park, T. A. Taton, C. A. Mirkin, *Science* **2002**, *295*, 651.
[11] M. Jiang, C. M. Cobley, B. Lim, Y. N. Xia, *Mater. Lett.* **2009**, *4*, 8.
[12] G. Schmid, *Chem. Rev.* **1992**, *92*, 1709.
[13] G. Schmid, B. Corain, *Eur. J. Inorg. Chem.* **2003**, 3081.
[14] D. Wang, T. Xie, Q. Peng, Y. D. Li, *J. Am. Chem. Soc.* **2008**, *130*, 4016.
[15] C. M. Niemeyer, *Angew. Chem.* **2001**, *113*, 4254; *Angew. Chem. Int. Ed.* **2001**, *40*, 4128.
[16] R. Xu, T. Xie, Y. Zhao, Y. Li, *Cryst. Growth Des.* **2007**, *7*, 1904.
[17] J. Chen, T. Herricks, Y. Xia, *Angew. Chem.* **2005**, *117*, 2645; *Angew. Chem. Int. Ed.* **2005**, *44*, 2589.
[18] M. A. Mahmoud, C. E. Tabor, M. A. El-Sayed, Y. Ding, Z. L. Wang, *J. Am. Chem. Soc.* **2008**, *130*, 4590.
[19] N. Zheng, J. Fan, G. D. Stucky, *J. Am. Chem. Soc.* **2006**, *128*, 6550.
[20] H. Song, F. Kim, S. Connor, G. A. Somorjai, P. D. Yang, *J. Phys. Chem. B* **2005**, *109*, 188.
[21] J. Luo, P. N. Njoki, Y. Lin, D. M. Wang, C. J. Zhong, *Langmuir* **2003**, *19*, 10081.
[22] J. Xu, T. Zhao, Z. Liang, L. Zhu, *Chem. Mater.* **2008**, *20*, 1688.
[23] S. Zhou, G. S. Jackson, B. Eichhorn, *Adv. Funct. Mater.* **2007**, *17*, 3099.
[24] L. Yang, W. Yang, Q. Cai, *J. Phys. Chem. C* **2007**, *111*, 16613.
[25] A. Cruz, E. Poulain, G. D. Angel, S. Castillo, V. Bertin, *Int. J. Quantum Chem.* **1998**, *67*, 399.
[26] V. Abdelsayed, A. Aljarash, M. S. El-Shall, *Chem. Mater.* **2009**, *21*, 2825.
[27] S. Zhou, K. Mcllwrath, G. Jackson, B. Eichhorn, *J. Am. Chem. Soc.* **2006**, *128*, 1780.
[28] J. Grunes, J. Zhu, G. A. Somorjai, *Chem. Commun.* **2003**, 2257.
[29] C. Shen, C. Hui, T. Yang, C. Xiao, J. Tian, L. Bao, S. Chen, H. Ding, H. Gao, *Chem. Mater.* **2008**, *20*, 6939.
[30] X. Lu, H. Tuan, J. Chen, Z. Li, B. A. Korgel, Y. Xia, *J. Am. Chem. Soc.* **2007**, *129*, 1733.
[31] X. Z. Lin, X. Teng, H. Yang, *Langmuir* **2003**, *19*, 10081.
[32] T. Shimizu, T. Teranishi, S. Hasegawa, M. Miyake, *J. Phys. Chem. B* **2003**, *107*, 2719.
[33] N. Toshima, Y. T. Yonezawa, *New J. Chem.* **1998**, *22*, 1179.
[34] S. W. Kim, J. Park, Y. Jang, Y. Chung, S. Hwang, T. Hyeon, Y. W. Kim, *Nano Lett.* **2003**, *3*, 1289.
[35] C. A. Stowell, B. A. Korgel, *Nano Lett.* **2005**, *5*, 1203.
[36] E. V. Shevchenko, D. V. Talapin, C. B. Murray, S. O'Brien, *J. Am. Chem. Soc.* **2006**, *128*, 3620.
[37] F. X. Redl, K. S. Cho, C. B. Murray, S. O'Brien, *Nature* **2003**, *423*, 968.
[38] A. Courty, C. Fermon, M. P. Pileni, *Adv. Mater.* **2001**, *13*, 254.
[39] S. U. Son, Y. Jang, K. Y. Yoon, E. Kang, T. Hyeon, *Nano Lett.* **2004**, *4*, 1147.
[40] G. Viau, R. Brayner, L. Poul, N. Chakroune, E. Lacaze, F. Fiévet-Vincent, F. Fiévet, *Chem. Mater.* **2003**, *15*, 486.
[41] T. Herricks, J. Chen, Y. Xia, *Nano Lett.* **2004**, *4*, 2367.
[42] J. D. Hoefelmeyer, K. Niesz, G. A. Somorjai, T. D. Tilley, *Nano Lett.* **2005**, *5*, 435.
[43] A. Tao, P. Sinsermsuksakul, P. Yang, *Angew. Chem.* **2006**, *118*, 4713; *Angew. Chem. Int. Ed.* **2006**, *45*, 4597.
[44] B. L. V. Prasad, S. L. Stoeva, C. M. Sorensen, K. J. Klabunde, *Langmuir* **2002**, *18*, 7515.
[45] B. L. V. Prasad, S. L. Stoeva, C. M. Sorensen, K. J. Klabunde, *Chem. Mater.* **2003**, *15*, 935.
[46] Y. Sun, Y. Xia, *J. Am. Chem. Soc.* **2004**, *126*, 3892.
[47] T. Teranishi, M. Miyake, *Chem. Mater.* **1998**, *10*, 594.
[48] Z. A. Peng, X. G. Peng, *J. Am. Chem. Soc.* **2001**, *123*, 1389.
[49] K. Bauer, D. Garbe, *Common Fragrance and Flavor Materials*, VCH, Weinheim, **1985**.
[50] C. Milone, M. L. Tropeano, G. Gulino, G. Neri, R. Ingoglia, S. Galvagno, *Chem. Commun.* **2002**, 868.
[51] B. Pawelec, A. M. Venezia, V. La Parola, E. Cano-Serrano, J. M. Campos-Martin, J. L. G. Fierro, *Appl. Surf. Sci.* **2005**, *242*, 380.
[52] F. Liu, D. Wechsler, P. Zhang, *Chem. Phys. Lett.* **2008**, *461*, 254.
[53] A. Baiker, *Chem. Rev.* **1999**, *99*, 453.
[54] F. Y. Zhao, S. Fujita, S. Akihara, M. Arai, *J. Phys. Chem. A* **2005**, *109*, 4419.
[55] F. Y. Zhao, S. Fujita, J. Sun, Y. Ikushima, M. Arai, *Chem. Commun.* **2004**, 2326.
[56] R. Liu, F. Zhao, S. Fujita, M. Arai, *Appl. Catal. A* **2007**, *316*, 127.
[57] Y. Akiyama, S. Fujita, H. Senboku, C. M. Rayner, S. A. Brough, M. Arai, *J. Supercrit. Fluids* **2008**, *46*, 197.

Received: November 30, 2009
Published online: April 21, 2010

